## SSDM2025-151798

## AMORPHOUS BONDING FOR IN-SPACE WELDING OF THERMOPLASTIC COMPOSITE DEPLOYABLE STRUCTURES

Cesar Moriel<sup>1,†,\*</sup>, Joseph G. Kirchhoff<sup>2,†</sup>, Miguel Mireles <sup>1</sup>, Tyler B. Hudson<sup>3</sup>, Mehran Tehrani<sup>4</sup>, Armanj D. Hasanyan<sup>1</sup>

<sup>1</sup>Department of Aerospace and Mechanical Engineering, The University of Texas at El Paso, El Paso, TX 79968

<sup>2</sup>Walker Department of Mechanical Engineering, The University of Texas at Austin, Austin, TX 78712

<sup>3</sup>NASA Langley Research Center, Hampton, VA, 23681

<sup>4</sup>Department of Structural Engineering, University of California San Diego, La Jolla, CA, 92093

#### **ABSTRACT**

To meet the demands for large-scale space structures and overcome the constraints of volume and weight, stowing segments of a deployable boom and welding in-space offers a possible solution. As a result, thin-ply thermoplastic polymer composites (TPCs) are analyzed in this study for their ability to undergo multiple welding cycles through fusion bonding, which consists of intimate contact, healing, and solidification. Crystallization of TPCs poses a challenge during thermoplastic processing, as it impairs interface healing and requires slow cooling to achieve proper fiber-matrix adhesion, which can be challenging for inspace welding. To address this, a composite material is developed by introducing an amorphous polyetherimide (PEI) sheath layer to the surfaces of a semi-crystalline polyetheretherketone (PEEK) composite. Notably, the sheath is miscible with and healable below the melt temperature of the PEEK, resulting in a thermoplastic composite capable of welding without melting the crystals, forming a 'Goldilocks Zone' for structural bonding. This research initiates an exploration of the potential of amorphous bonding for deployable space structures, by presenting a series of material tests. The details of the fabrication of the new thin-ply TPC are discussed and large-curvature Column Bending Test (CBT) results are presented. CBTs are conducted to assess the effect of the additional amorphous PEI layer on bending stiffness, failure curvature, and failure modes in the large-curvature regime. The results show promise for amorphous bonding of deployable structures in-space.

# Keywords: Thermoplastics, Deployable Structures, Column Bending Test (CBT), In-Space Welding

#### 1. INTRODUCTION

Deployable structures are designed to be coiled into a compact form for stowage and deploy to a functional configuration in-space. Common deployables, such as the Triangular Rollable and Collapsible (TRAC) longerons [1] and the Collapsible Tubular Mast (CTM) booms [2], are composed of two independent tape spring-like sections bonded together at the web-region. Although these cross-sectional geometries provide efficient structural support when deployed, the kinematic mismatch at the web provides a shear-lag zone during coiling that induces the formation and propagation of localized buckling folds. The mechanisms for the kinematic mismatch is outlined in [3] and the corresponding failure modes as a result of these are discussed in [1] and [4].

To prevent these failure modes, large factors of safety are typically introduced on the coiling radius of these structures. Tape spring structures, which do not have a web-region and the kinematic mismatch associated with them have a much smaller coiling radius. As a result, stowing the segments of the TRAC longeron or the STM boom separately and bonding them at the web region post-deployment can provide a more-efficient delivery approach.

Thermoplastic polymer composites (TPCs) may be well-suited for these applications for their ability to undergo multiple bonding cycles. For space structural applications, thin-ply TPCs have been previously discussed for their high toughness, creep resistance and temperature stability [5]. Schlothauer et al. [6] found that thin (35  $\mu$ m) T700/PEEK measured a 66% improvement in transverse strength compared to conventional thermoset epoxy systems used in deployable structures. Building on the mechanical advantages of TPCs discussed earlier, this study also investigates their weldability, with a particular focus on the use of multiple polymers in the composites.

Amorphous bonding refers to the idea of using amorphous

<sup>†</sup>Joint first authors

<sup>\*</sup>Corresponding author: cemoriel2@miners.utep.edu

polymers at the bonding interface of semi-crystalline composites. The motivation for amorphous bonding lies within the intricacies of thermoplastic fusion bonding which involves intimate contact, healing (interdiffusion or autohesion), and solidification [7]. Intimate contact refers to the development of polymer-polymer contact or the removal of surface roughness at the interface [8]. Polymer healing occurs upon intimate contact in an amorphous state [9]. In semi-crystalline polymers, the melting temperature  $(T_m)$  refers to state transition to an amorphous phase [10]. It has been shown that the presence of crystallinity prevents polymer healing through thoughtful rheometry experiments [11]. The implication is that the semi-crystalline polymer healing ceases upon crystallization during solidification reducing the processing window [12]. Moreover, to weld a semi-crystalline polymer the crystals must be melted first. Amorphous polymers heal above their glass transition temperatue  $(T_g)$  while semi-crystalline polymers heal above their  $T_m$ .

In the 1990s, amorphous bonding was first investigated as a dual-bonding process called Thermabond where amorphous polyetherimide (PEI) was fusion bonded to the surface of a carbon fiber (CF) PEEK laminate. A 100  $\mu m$  layer of PEI was healed to one side of the laminate via hot pressing, forming a sheath, and then two laminates were welded together using the sheaths [13, 14]. The key benefit of the added PEI is that healing can occur below the melt temperature of the PEEK such that the existing crystallinity does not get erased. Remarkably, the laminates can be welded while maintaining thermal geometric stability as well. There is limited literature of amorphous bonding, but there has been recent efforts to develop PEEK-PEI prepreg tapes for high-rate applications [15]. This study investigates developing thin PEEK composite laminates with PEI sheaths specifically for inspace welding of deployable structures.

This study outlines a method for manufacturing thermoplastic segments with amorphous bonding surfaces. During the production of individual segments, an amorphous polymer can be incorporated into the layup and consolidated with the semi-crystalline composite above the melt temperature. Possible manufacturing techniques include continuous compression molding and vacuum bagging. The individual segments can then be stored without concerns of non-smooth coiling, allowing for tighter, more conformable radii. Upon deployment, a welding procedure could be employed to heat the bonding interfaces to the 'Goldilocks Zone'—the temperature range where the amorphous polymer can bond and heal without deforming the semi-crystalline polymer. Additionally, because the amorphous polymer is not constrained by cooling rates, nor were the crystals ever melted, this potential issue is effectively mitigated leading to a cooling rate independent welding process.

### 2. METHODOLOGY

The semi-crystalline (PEEK) prepreg used was Toray's Cetex TC1200 with AS4 fibers, with a nominal thickness of  $125\mu m$ . The amorphous film (PEI) used was sourced from CS Hyde with a nominal thickness of  $25\mu m$ . The film thickness is an important factor for ensuring there is sufficient amorphous polymer for bonding with minimal reduction of the local fiber-volume fraction.  $[PEI/0_3/PEI]$  and [PEI/0/90/0/PEI] laminates were

prepared using a vacuum bag process in an oven. The high temperature bagging materials were supplied by Airtech, namely Thermalide (with two coats of Frekote applied) for the vacuum bag and release material. The breather material used was Airweave UHT 300PGL. The vacuum bag configuration consisted of Thermalide  $\rightarrow$  laminate  $\rightarrow$  Thermalide (two layers)  $\rightarrow$  Breather  $\rightarrow$  Thermalide (Vacuum). Under vacuum pressure, the samples were consolidated at 380°C for 30 minutes and then cooled at 5°C/min to ensure sufficient crystal growth in the PEEK. To fusion bond PEI and PEEK together, both polymers need to be in an amorphous state (> $T_m$  of the PEEK). The resultant laminate thickness was  $\sim$  0.44 mm.

## 2.1 Thermal Stability - Dynamic Mechanical Analysis

Dynamic Mechanical Analysis (DMA) was performed in a three-point bending configuration to evaluate the flexural modulus of the material at elevated temperatures. The objective was to identify a temperature window in which PEI could effectively bond with other segments without compromising the shape of the PEEK-CF composite. The test was conducted using a Netzsch DMA 242 E Artemis. A  $20.0\times1.1\times\sim0.40~mm$  sample was cut from the  $[PEI/0_3/PEI]$  laminate using a wet saw. With a constant 1Hz frequency, a displacement amplitude of  $25~\mu m$  was applied from 30 to  $400^{\circ}$ C at  $5^{\circ}$ C/min.

## 2.2 Column Bending Test (CBT)

To accurately characterize the high-curvature bending behavior of thin laminates, including their failure curvature, a specialized testing method is required to subject thin composite laminates to extreme curvatures, often exceeding 0.4 mm<sup>-1</sup> [16]. Traditional bending tests, such as three- and four-point bending, are limited to the linear deformation regime and therefore inadequate for this purpose [17]. Alternative methods have been investigated to address these limitations. The platen test has been used to measure the failure curvature of thin laminates [18], but the non-uniform moment distribution across the sample introduces significant errors in data interpretation unless the complex deformation behavior is meticulously modeled. Similarly, the four-point large-deformation bend test can achieve the required high curvatures; however, the sharp change in stress distribution in the grips often causes premature failure of the test specimens [19].

The Column Bending Test (CBT), developed by Murphey and Fernandez [17], combines the benefits of both the platen test and large-deformation four-point bending tests. This setup generates a stress distribution that peaks at the mid-gauge section of the sample, similar to the platen test, but decreases only slightly (to around 80-90% of the maximum stress) near the grips [17]. A significant advantage of the CBT is its nearly uniform bending moment distribution, which results in a constant curvature across the specimen. This uniformity simplifies the analysis, allowing for straightforward interpretation using geometric principles [16]. Furthermore, the reduced curvature near the grips minimizes grip-induced failure, making the mid-region of the sample more likely to fail. This characteristic makes the CBT particularly effective for studying material behavior in large-deformation

bending scenarios, while ensuring accurate and reproducible results.

The CBT is used to assess the flexural stiffness and failure properties of thin laminate flexures in pure bending conditions. It specifically measures the moment-curvature response and failure curvature of high-strain composites (HSC) in the large-curvature regime ( $k = 0.12 \text{ mm}^{-1}$ ). The slope of the moment-curvature curve yields the bending stiffness ( $D_{11}$ ) for the chosen laminate layout, which is directly proportional to the applied curvature. Analyzing these curves additionally shows material nonlinearities and the progressive failure behavior of the tested coupons. The purpose of this subsection is to characterize the closed-form relationships between displacement and curvature, as well as force and moment, in the CBT, assuming uniform curvature across the test sample.

The CBT fixtures used in this research were the same to those described by [20]. These aluminum fixtures were designed for compatibility with an Instron testing machine. The setup features a U-shaped clevis attached to the extension head of the Instron machine, with a rigid arm connected to the center of the clevis via a rigid rod. Bearings were incorporated into the design to minimize friction between the rod, arm, and clevis as seen in Fig. 1a. During testing, the top fixture moved toward the bottom fixture at a displacement rate of 10 mm/min as seen in Fig. 1b, while folding forces were measured using a 500 N load cell.

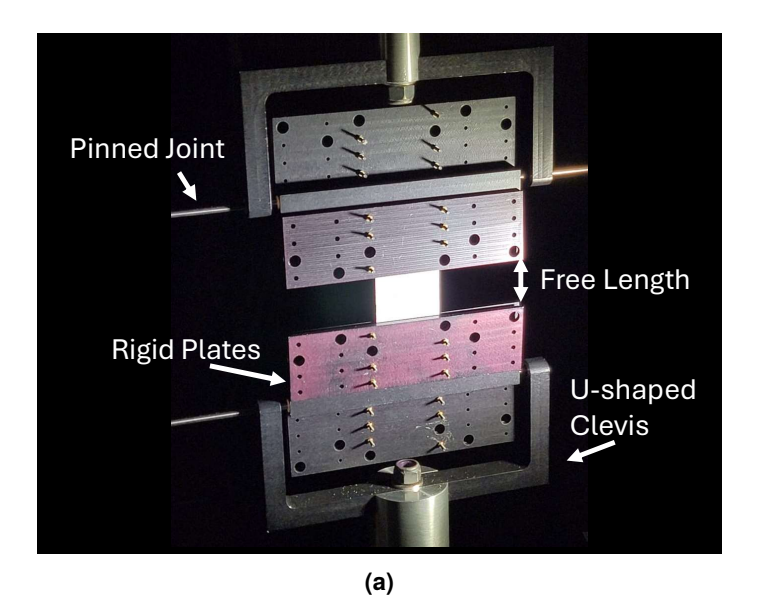
Strain and curvature distributions were recorded using a single-side dual-camera system paired with 3D Stereo Digital Image Correlation (DIC) software, capturing images at a rate of 1 frame per second. To measure both tension and compression surface strains, the fixtures were flipped, allowing for data collection from both sides of the samples, tension and compression surface.

The specimen was secured to the arm using bolts and a rigid plate, leaving a free length (l) between the two rigid fixtures. The sample was clamped to the top and bottom surfaces of the arms using rigid plates. The CBT fixture design includes horizontal and vertical offsets of 5.1 mm and 37.5 mm, respectively. The samples were prepared with a black-and-white acrylic speckle pattern to create a high contrast pattern. A roller was used to apply the pattern, with black speckles having a dot size of 0.18 mm. Various subset and step sizes were tested to determine the optimal configuration, resulting in the selection of a subset size of 37 and a step size of 17, which produced the least amount of noise in the analysis.

The samples were cut to dimensions of 60 mm  $\times$  30 mm, utilizing a diamond saw, providing sections of 20 mm for clamped/free-length/clamped regions. A sandpaper layer was adhered to the clamped regions between the sample and the fixtures to prevent failure at the grips. The selected free length was designed to achieve a desired curvature of  $k=0.12~{\rm mm}^{-1}$ . To attain a higher curvature, the free length must be reduced; however, due to the relatively substantial thickness of our laminates  $(t=0.44~{\rm mm})$ , a larger free length was chosen. Two laminates were subjected to testing using the Column Bending Test (CBT).

1.  $[PEI/0_3/PEI]$ : A unidirectional laminate that provides insights into the axial stiffness and strength, simulating the

- primary load-bearing direction in a deployable structure.
- 2. [PEI/0/90/0/PEI]: A balanced laminate that offers a combination of axial and transverse stiffness, representative of structures experiencing multi-directional loads.



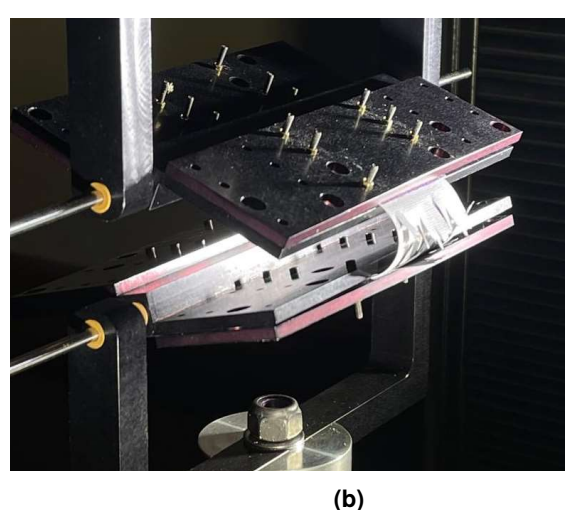


FIGURE 1: (A) INITIAL AND (B) LOADED CONFIGURATIONS OF THE CBT.

## 3. RESULTS

Thin semi-crystalline thermoplastic composites with amorphous bonding surfaces were tested with the CBT in the large curvature domain. This is to verify if the amorphous polymer influences the behavior. DMA was conducted to verify the thermal stability of the semi-crystalline composite at welding temperatures of the amorphous coating. Optical images of the cross-sections were taken to evaluate at the microstructure of the laminates.

### 3.1 DMA Results

The motivation for incorporating the amorphous polymer is to enable thermal welding of the segments without altering

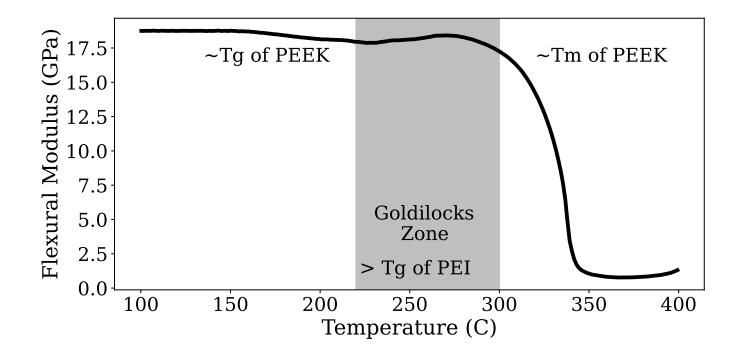


FIGURE 2: DYNAMIC MECHANICAL ANALYSIS CONDUCTED IN THREE-POINT BENDING AT A CONSTANT 1HZ FREQUENCY FOR A 25  $\mu m$  DISPLACEMENT AMPLITUDE.

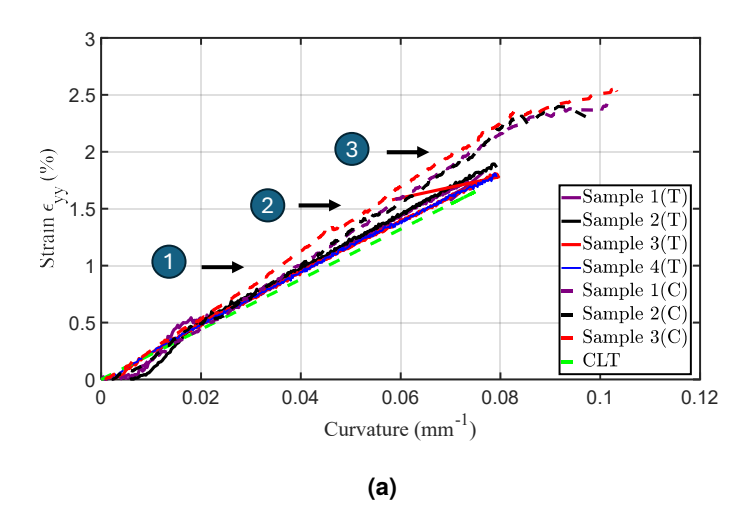
their geometric integrity. In many cases, the geometry of the segments is critical to their functionality — such as in the case of omega-shaped booms — and it is essential to avoid warping or deformation during the welding process to preserve their intended shape and performance. DMA results are shown in Figure 2. The force required to cause a displacement amplitude of  $25 \, \mu m$  at a constant frequency of 1 Hz was measured through  $400^{\circ}C$ . Surprisingly, the flexural modulus decreases significantly around  $300^{\circ}C$ , which is approximately  $40^{\circ}C$  lower than the reported  $T_m$  of PEEK in the literature [10]. Fortunately, PEI can weld above its  $T_g$  of  $220^{\circ}C$ , with welding times ranging from 0.7 to 3 seconds at  $320^{\circ}C$  and from 63 to 321 seconds at  $300^{\circ}C$  [21]. This 'Goldilocks Zone' (PEI can be healed without deforming the PEEK) is promising for in-space welding of thermoplastic segments through amorphous bonding.

#### 3.2 CBT Results

To evaluate the behavior of thin composite materials consisting of an amorphous PEI sheath on the surface of semi-crystalline PEEK composites under pure bending, force-curvature relationships and strain data obtained from DIC were analyzed.

The surface strain results for both compression and tension sides of the [PEI/0<sub>3</sub>/PEI] laminate are presented in Fig. 3a. It is noteworthy that the compression samples (C) attained a strain of approximately 3\%, whereas the tension samples (T) exhibited values ranging between 2% and 2.4%, despite identical testing conditions. This observation underscores that the compression surface strain consistently exceeds the tension surface strain. Furthermore, the linear material behavior, as predicted by the Classical Lamination Theory (CLT), is depicted in green in Fig. 3a, illustrating how the non-linear behavior of the fibers begins to deviate from the linear prediction at a curvature of approximately 0.04 mm<sup>-1</sup> for the compression surface strain while for the tension surface strain it remains closer. This deviation falls within the same range reported by Murphey in [17], where most samples demonstrated a 10% difference with the CLT, while some remained within a 50% difference range.

As illustrated in Fig. 3b, the strain distribution is quasiuniform across the sample which validates the test parameters and procedure; however, edge effects are apparent, influencing strain measurements in proximity to the edges.



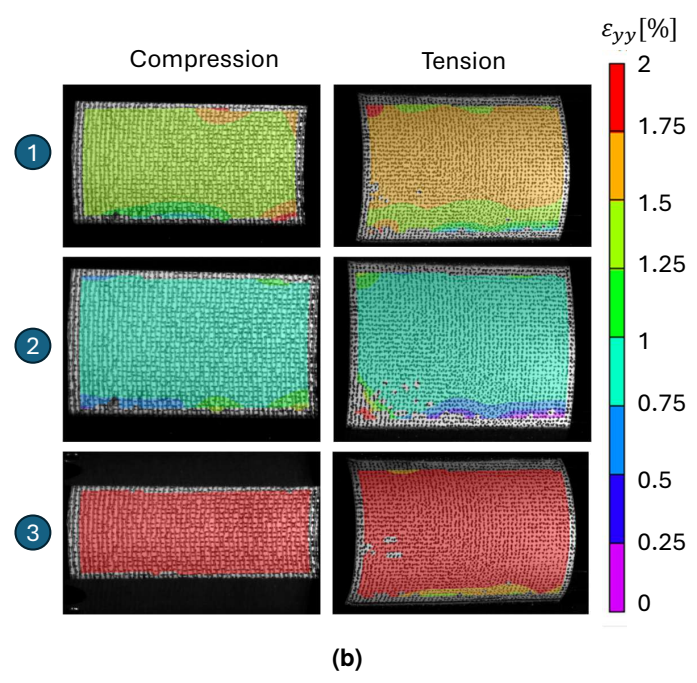


FIGURE 3: (A) PEI/0 $_3$ /PEI LAYUP WITH A 20 MM FREE LENGTH: STRAIN ( $\epsilon_{yy}$ ) VS. CURVATURE, AND (B) STRAIN DISTRIBUTION ACROSS THE SAMPLE AT VARIOUS STRAIN LEVELS.

The required resultant moment versus the curvature of the layup [PEI/0<sub>3</sub>/PEI] is shown in Fig. 4a for both compression and tension surfaces. Notably, failure is more abrupt on the tension side, where it begins to manifest at approximately  $k = 0.85 \, \mathrm{mm}^{-1}$ . In contrast, the compression side requires a larger curvature of approximately  $k = 0.95 \, \mathrm{mm}^{-1}$  to observe failure. Despite this, the required resultant moment remained within the same range of approximately 63 to 70 N. The units of the resultant moment are expressed in N because the moment, originally in N-mm, is divided by the width (30 mm), resulting in N-mm/mm = N.

As shown in Fig. 4b, the curvature distribution across the sample is nearly uniform, with the only gaps in data attributed to the speckle pattern. This supports the validity of the test parameters and confirms the assumption of uniform curvature and strain in the CBT. Uniform curvature and strain were consistently achieved across all samples of both laminates.

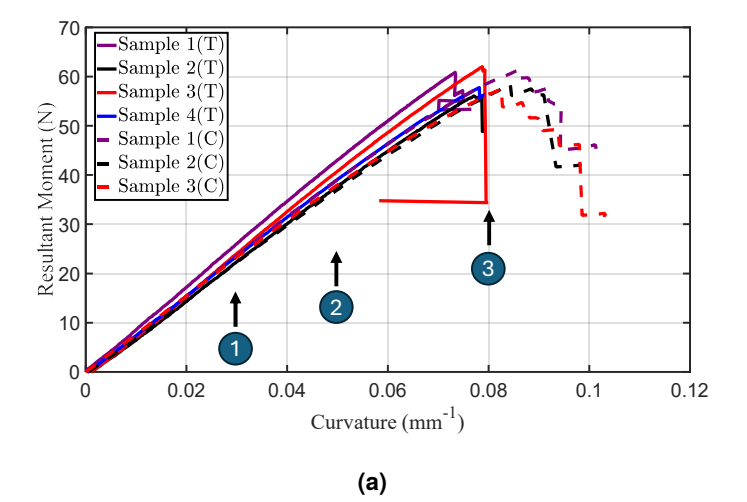
As illustrated in Fig. 5, the bending stiffness ( $D_{11}$ ) calculated from the compression side shows a smaller percentage difference compared to the tension side. The units of bending stiffness are expressed in N-mm because it is defined as the resultant moment (in N) divided by the curvature (in 1/mm), resulting in N-mm. The results on the tension side show a higher average bending stiffness of about 750 N-mm  $\pm$  37.4 N-mm, while those from the compression side are more consistent, averaging around 706 N-mm  $\pm$  15.9 N-mm.

The surface strain results for both the compression and tension sides of the [PEI/0/90/0/PEI] laminate are shown in Fig. 6. Notably, the compression samples (C) reached strain levels between approximately 1.35% and 1.9%, which is significantly lower—nearly half—than the strain observed in the [PEI/0<sub>3</sub>/PEI] laminate. On the other hand, the tension samples (T) displayed strain values ranging from 1.2% to 1.6%, aligning more closely with the results from this laminate. This comparison highlights that the compression surface strain consistently exceeds the tension surface strain previously reported.

Additionally, the green line in Fig. 6 represents the linear material behavior predicted by Classical Lamination Theory (CLT). It is evident that the non-linear behavior of the fibers causes a noticeable deviation from the linear prediction at a curvature of approximately  $0.01~\mathrm{mm}^{-1}$  for the compression and the tension surface strain.

The relationship between the resultant moment and curvature for the [PEI/0/90/0/PEI] layup on both the tension (T) and compression (C) surfaces is shown in Fig. 7a. Failure is observed to occur abruptly, with the resultant moment dropping to zero almost instantaneously, as captured within a single frame at rate of 1 frames per second (FPS). For the tension samples, failure initiation is broadly observed within a curvature range of  $k = 0.045 \text{ mm}^{-1}$  to  $k = 0.057 \text{ mm}^{-1}$ , while for the compression samples, the range extends from  $k = 0.048 \text{ mm}^{-1}$  to  $k = 0.065 \text{ mm}^{-1}$ .

Throughout these ranges, the required resultant moment for the tension samples remains relatively stable, fluctuating between 38 and 45 N. In contrast, the compression samples exhibit a wider range of resultant moments, spanning from 32 to 52 N. This variation could potentially be attributed to inherent manufacturing flaws, which are particularly critical in thin-ply composites.



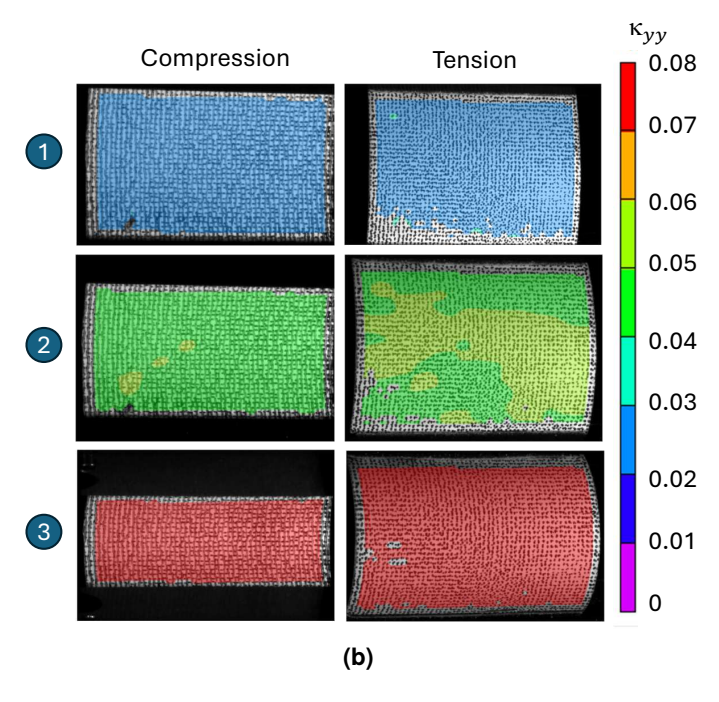


FIGURE 4: (A) PEI/0 $_3$ /PEI LAYUP WITH A 20 MM FREE LENGTH: RESULTANT MOMENT (N) VS. CURVATURE, AND (B) CURVATURE DISTRIBUTION ACROSS THE SAMPLE AT VARIOUS STRAIN LEVELS.

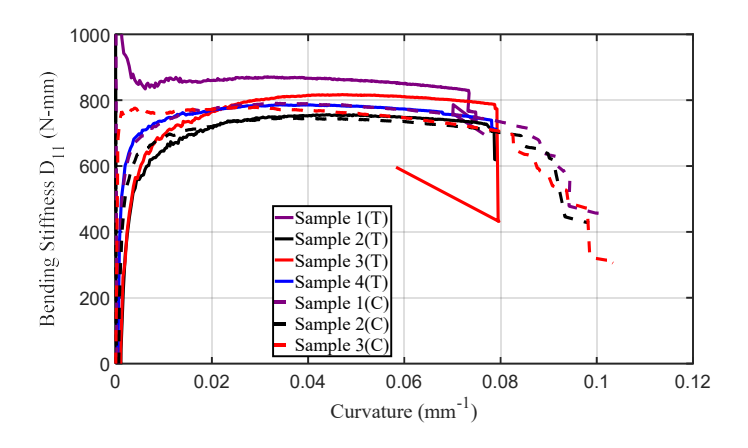


FIGURE 5:  $PEI/0_3/PEI$  LAYUP WITH A 20 MM FREE LENGTH: BENDING STIFFNESS ( $D_{11}$ ) VERSUS CURVATURE FOR TENSION (T) AND COMPRESSION (C) SURFACES.

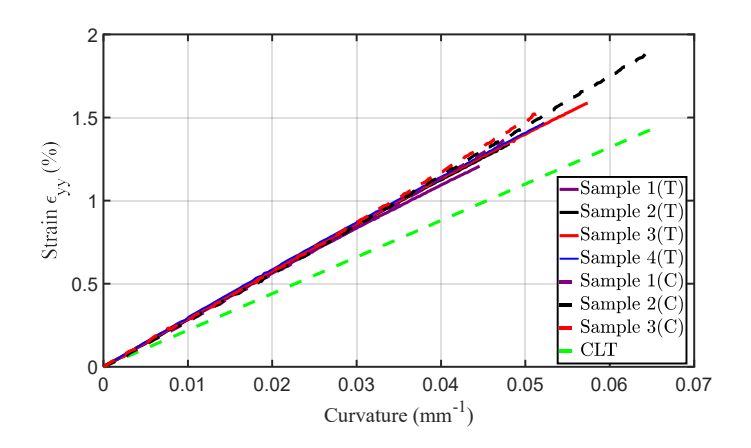
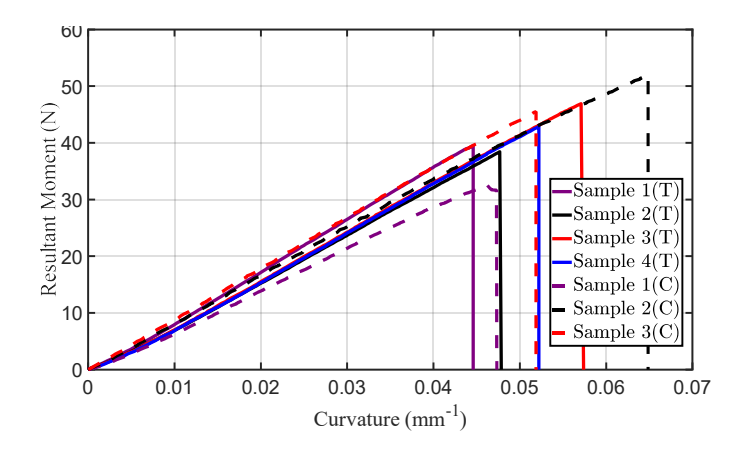


FIGURE 6: PEI/0/90/0/PEI LAYUP WITH A 20 MM FREE LENGTH: STRAIN  $(\epsilon_{\gamma\gamma})$  VS. CURVATURE.

Even though the resultant moment versus curvature relationship reveals some variation in critical failure parameters, the bending stiffness  $(D_{11})$  derived from the tension side exhibits greater consistency, as shown in Fig. 7b. For the tension samples,  $D_{11}$  had an average of 835 N-mm  $\pm$  35 N-mm. In contrast, the compression samples display a wider range of bending stiffness values, with an average of 816 N-mm  $\pm$  88.7 N-mm.

Fig. 8a illustrates the failure mode of the [PEI/0<sub>3</sub>/PEI] laminate on the tension side, where surface delamination is prominently observed at the center of the specimen. In contrast, Fig. 8b shows the failure mode on the compression side, with significantly less surface delamination compared to the tension side. Fiber-matrix splitting is more pronounced on the tension side, particularly in the first and fourth samples (from left to right), where vertical, straight-line cracks aligned with the fiber direction are evident. Notably, sample 1 on the compression side shows no visible damage, while all tension-side samples exhibit clear signs of failure.

Similarly, Fig. 9a illustrates the failure of the [PEI/0/90/0/PEI] laminate on the tension side, exhibiting catastrophic failure predominantly at the center of the specimen. This observation aligns with Fig. 9b, which depicts the catas-



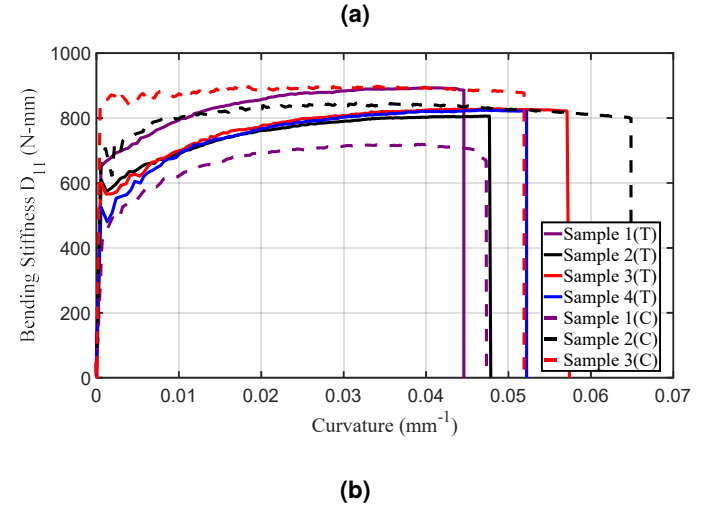
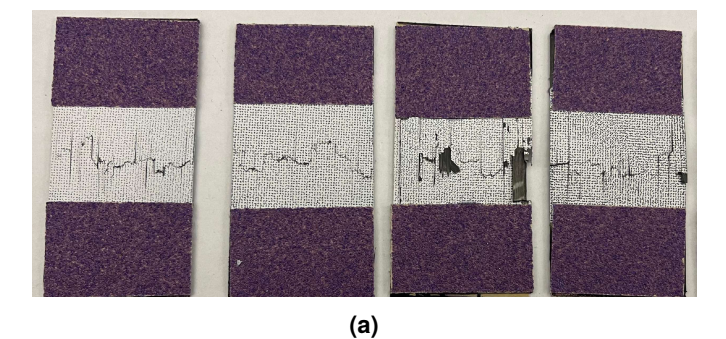


FIGURE 7: PEI/0/90/0/PEI LAYUP WITH A 20 MM FREE LENGTH, SHOWING RESULTS FROM BOTH THE TENSION SURFACE: (A) RESULTANT MOMENT VERSUS CURVATURE AND (B) BENDING STIFFNESS ( $D_{11}$ ) VERSUS CURVATURE.

trophic failure of the compression-side samples, also occurring primarily at the midpoint of the specimen. While the majority of samples failed directly at the center, a few exhibited failure closer to the region between the edge and the midpoint.

### 4. CONCLUSION & DISCUSSION

The potential of PEEK/CF with resin-rich PEI surfaces for inspace welding of deployable structures has been investigated. The amorphous PEI is fusion bonded to the semi-crystalline PEEK during initial manufacturing of the laminates (or deployable segments). The PEI and PEEK are miscible, forming a cohesive interface, and notably, PEI-PEI welding can occur at temperatures below the melt temperature of PEEK. DMA confirmed the existence of a 'Goldilocks Zone' for this process, with a temperature range of approximately  $\sim 220^{\circ}\text{C} \rightarrow 300^{\circ}\text{C}$ . PEI requires less time to weld at higher temperatures (< 1 second at 320°C), suggesting that using a semi-crystalline polymer with a higher melting point would improve this concept further. Amorphous bonding yields special promise for improving the feasibility of welding segments of deployable structures in space without warping the structure. Stowing the segments separately would



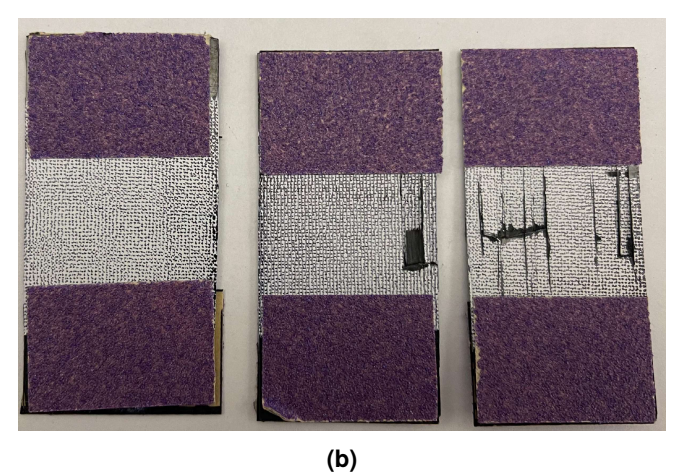
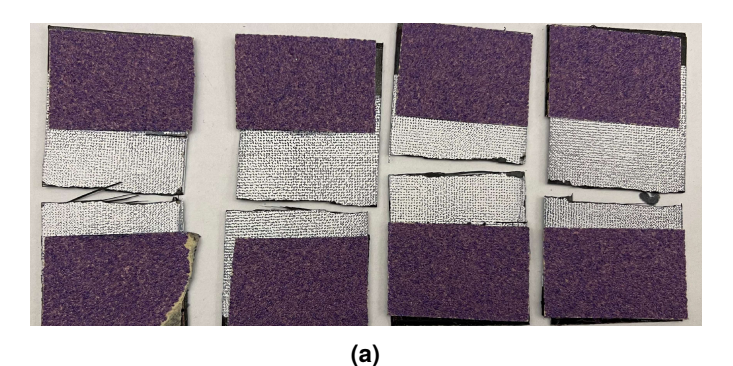


FIGURE 8:  $PEI/0_3/PEI$  LAYUP FAILURE MODE AT THE (A) TENSION AND (B) COMPRESSION SURFACES.

maximize the weight-to-volume ratio upon launch. CBT was performed to confirm that the resin-rich interfaces do not compromise the large curvature behavior of PEEK/CF composites. Stereo-DIC analysis revealed that, despite high surface strains, the amorphous polymer did not fail prematurely, with the laminate ultimately experiencing catastrophic fiber-matrix splitting rather than failure at the resin-rich interfaces. The  $[PEI/0_3/PEI]$ laminate reached a strain of approximately 1.2% during loading, while the [PEI/90/0/90/PEI] laminate stayed below 0.7%. Although the  $[PEI/0_3/PEI]$  laminate approached higher strain levels, it fell short of the 2% strain typically desired for deployable structures. The laminate's excessive thickness (approximately  $440 \,\mu\text{m}$ ) is likely a contributing factor. Investigating thinner laminates (around 35  $\mu$ m) with amorphous surfaces is essential to achieving the strain levels required for deployable structure applications. Future research should also focus on demonstrating the conductive welding of two segments within the 'Goldilocks Zone'. This study is the first to explore amorphous bonding for deployable structures, highlighting its potential and justifying future work in this area.

#### **ACKNOWLEDGMENTS**

The authors are grateful for Joseph Kirchhoff's support provided by NASA NSTGRO grant #80NSSC22K1203. A special thank you to Wilfredo Flores for manufacturing the laminates and to Gehan Jayatilaka for assistance with the DMA.



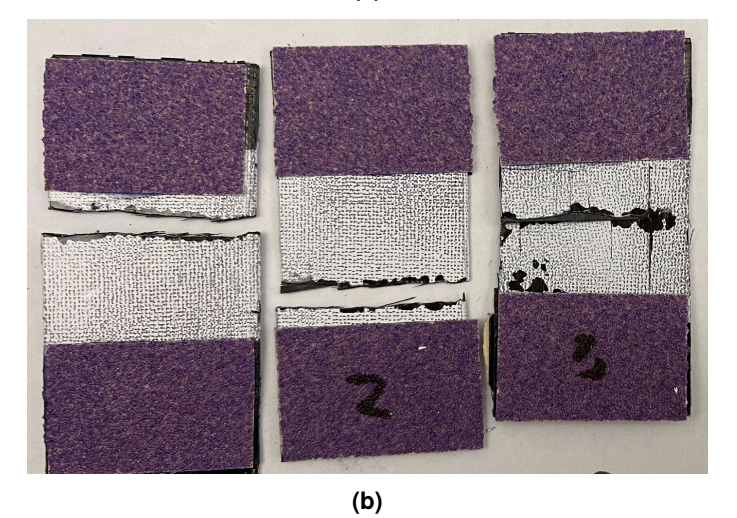


FIGURE 9: PEI/0/90/0/PEI LAYUP FAILURE MODES AT THE (A) TENSION AND (B) COMPRESSION SURFACES.

#### **REFERENCES**

- [1] Leclerc, Christophe, Wilson, Lee, Bessa, Miguel A. and Pellegrino, Sergio. "Characterization of ultra-thin composite triangular rollable and collapsible booms." *4th AIAA Spacecraft Structures Conference*, 2017. 2017. American Institute of Aeronautics and Astronautics Inc, AIAA. DOI 10.2514/6.2017-0172.
- [2] Stohlman, Olive R, Zander, Martin E and Fernandez, Juan M. "Characterization and modeling of large collapsible tubular mast booms." *AIAA Scitech 2021 Forum*: p. 0903, 2021.
- [3] Luo, Wen and Pellegrino, Sergio. "Formation and propagation of buckles in coilable cylindrical thin shells with a thickness discontinuity." *International Journal of Solids and Structures* Vol. 259 (2022): p. 112010.
- [4] Hasanyan, Armanj D and Pellegrino, Sergio. "Modeling of Damage in Coilable Composite Shell Structures." *AIAA Scitech 2023 Forum*: p. 0364. 2023.
- [5] Leif A. Carlsson, Donald F. Adams and R. Byron Pipes. Experimental Characterization of Advanced Composite Materials, 4th Edition (2002). URL https://books.google.com/books?hl=en&lr=&id=vBDlAgAAQBAJ&oi=fnd&pg=PP1&dq=info: ioYvxZQqyk0J:scholar.google.com&ots=63F6pXRKJr&sig=\_NCFXm7shnzyNICHX1qKqxzGHkY#v=onepage&q&f=false.

- [6] Schlothauer, Arthur, Schwob, Nicolas, Pappas, Georgios A. and Ermanni, Paolo. "Ultra-thin thermoplastic composites for foldable structures." AIAA Scitech 2020 Forum, Vol. 1 PartF. 2020. American Institute of Aeronautics and Astronautics Inc, AIAA. DOI 10.2514/6.2020-0206.
- [7] Ageorges, C, Ye, L and Hou, M. "Advances in fusion bonding techniques for joining thermoplastic matrix composites: a review." Technical report no. URL www.elsevier.com/locate/compositesa.
- [8] Lee, Woo IL, Sang Namdo, Kyung and Springer, George S. "A Model of the Manufacturing Process of Thermoplastic Matrix Composites Republic of Korea." Technical report no. 1987.
- [9] De Gennes, P G and Leger, L. "DYNAMICS OF ENTANGLED POLYMER CHAINS Further ANNUAL REVIEWS." *Ann. Rev. Phys. Chem* Vol. 33 (1982): pp. 49–61. URL www.annualreviews.org.
- [10] Velisaris, Chris N. and Seferis, James C. "Crystallization kinetics of polyetheretherketone (peek) matrices." *Polymer Engineering & Science* Vol. 26 No. 22 (1986): pp. 1574–1581. DOI 10.1002/PEN.760262208. URL https://onlinelibrary.wiley.com/doi/full/10.1002/pen.760262208https://onlinelibrary.wiley.com/doi/abs/10.1002/pen.760262208https://4spepublications.onlinelibrary.wiley.com/doi/10.1002/pen.760262208.
- [11] Boiko, Yuri M, Ârald, Ge, Ârin, Gue, Marikhin, Vyacheslav A and Prud'homme, Robert E. "Healing of interfaces of amorphous and semi-crystalline poly(ethylene terephthalate) in the vicinity of the glass transition temperature." *Polymers* Vol. 42 (2001). URL www.elsevier.com/locate/polymer.
- [12] Barocio, Eduardo, Brenken, Bastian, Favaloro, Anthony and Pipes, R. Byron. "Interlayer fusion bonding of semi-crystalline polymer composites in extrusion deposition additive manufacturing." *Composites Science* and Technology Vol. 230 (2022): p. 109334. DOI 10.1016/J.COMPSCITECH.2022.109334.
- [13] Smiley, A. J., Halbritter, A., Cogswell, F. N. and Meakin, P. J. "Dual polymer bonding of thermoplastic composite

- structures." *Polymer Engineering & Science* Vol. 31 No. 7 (1991): pp. 526–532. DOI 10.1002/pen.760310709.
- [14] Meakin, P J, Cogswell, F N, Halbritter, A J, Smiley, A J and Staniland, P A. "Thermoplastic interlayer bonding of aromatic polymer composites-methods for using semi-crystallized polymers." Technical report no.
- [15] Baho, Omar, Ausias, Gilles, Grohens, Yves, Barile, Marco, Lecce, Leonardo and Férec, Julien. "Automated fibre placement process for a new hybrid material: A numerical tool for predicting an efficient heating law." Composites Part A: Applied Science and Manufacturing Vol. 144 (2021). DOI 10.1016/j.compositesa.2021.106360.
- [16] Sharma, Ajay H, Rose, TJ, Seamone, Andrew, Murphey, Thomas W and Lopez Jimenez, Francisco. "Analysis of the column bending test for large curvature bending of high strain composites." AIAA scitech 2019 forum: p. 1746. 2019.
- [17] Fernandez, Juan M and Murphey, Thomas W. "A simple test method for large deformation bending of thin high strain composite flexures." 2018 AIAA spacecraft structures conference: p. 0942. 2018.
- [18] Yee, Jeffrey and Pellegrino, Sergio. "Biaxial bending failure locus for woven-thin-ply carbon fibre reinforced plastic structures." 46th AIAA/ASME/ASCE/AHS/ASC structures, structural dynamics and materials conference: p. 1811. 2005.
- [19] Sanford, Gregory E, Ardelean, Emil V, Murphey, Thomas W and Grigoriev, Mikhail M. "High strain test method for thin composite laminates." *16th International Conference on Composite Structures. Porto, Portugal.* 2011.
- [20] Mireles, Miguel and Hasanyan, Armanj. "Analysis of Stress Concentration Effects in High Strain Composite Column Bending tests Fixturex." (2024).
- [21] Barroeta Robles, J., Dubé, M., Hubert, P. and Yousefpour, A. "Healing study of poly (ether-imide) and poly ether ether ketone using resin films and a parallel plate rheometer." *Composites Part A: Applied Science and Manufacturing* Vol. 174 (2023). DOI 10.1016/j.compositesa.2023.107736.